Muon spin rotation and relaxation study of Ba$_2$CoO$_4$

Peter L. Russo,[1] Jun Sugiyama,[2] Jess H. Brewer,[3,*] Eduardo J. Ansaldo,[1] Scott L. Stubbs,[4] Kim H. Chow,[5] Rongying Jin,[6] Hao Sha,[7] and Jiandi Zhang[7]

[1]*TRIUMF, 4004 Wesbrook Mall, Vancouver, British Columbia, Canada V6T 2A3*
[2]*Toyota Central Research and Development Laboratories Inc., Nagakute, Aichi 480-1192, Japan*
[3]*CIfAR, TRIUMF and Department of Physics and Astronomy, University of British Columbia, Vancouver, British Columbia, Canada V6T 1Z1*
[4]*Department of Physics and Astronomy, University of British Columbia, Vancouver, British Columbia, Canada V6T 1Z1*
[5]*Department of Physics, University of Alberta, Edmonton, Alberta, Canada T6G 2G7*
[6]*Materials Science and Technology Division, Oak Ridge National Laboratory, Oak Ridge, Tennessee 37831, USA*
[7]*Department of Physics, Florida International University, Miami, Florida 33199, USA*

A positive muon spin rotation and relaxation (μ^+SR) experiment on a single crystal of Ba$_2$CoO$_4$ indicates the existence of an antiferromagnetic (AF) transition occurring at $T_N \approx 24$ K. Weak transverse field measurements show that the paramagnetic volume fraction of the sample decreases rapidly at the magnetic transition, indicating a bulk effect which cannot be due to the presence of impurities. Zero-field measurements reveal the presence of a magnetically ordered state below T_N with at least three crystallographically inequivalent muon sites. The results are compared to recent magnetic susceptibility and neutron measurements. Of the two AF spin structures proposed to explain recent neutron experiments, the μ^+SR results clearly exclude the one involving AF order along the c axis while supporting that with AF order in the ab plane.

I. INTRODUCTION

The cobalt ion in the cobalt oxides, with its multitude of possible valence states, plays an essential role in inducing the impressive range of phenomena found in these materials, including spin-state transitions in the perovskite LaCoO$_3$,[1,2] good thermoelectric performance in Na$_x$CoO$_2$ with $x \sim 0.7$,[3] superconductivity in Na$_{0.35}$CoO$_2$*yH$_2$O,[4] and two-dimensional (2D) antiferromagnetic (AF) order below 100 K in the quasi-one-dimensional (Q1D) cobalt oxide Ca$_3$Co$_2$O$_6$.[5] In these crystals the cobalt ions are located in CoO$_6$ octahedra and, as a consequence, experience a crystalline electric field (CEF) splitting between the t_{2g} and e_g levels of a few hundred Kelvin. As a result, the spin states of the Co^{3+} and Co^{4+} ions are very sensitive to T, with the low-spin configuration (LS) being the ground state at low T.

This sensitivity of the spin state to temperature directly leads to the spin-state transitions in LaCoO$_3$ and related perovskites and increases the degeneracy of the spin and orbital degrees of freedom of Co ions, which enhances thermopower in Na$_x$CoO$_2$ at high T.[6] Furthermore, the low-spin Co^{4+} ions with $S=1/2$ stabilize a spin-spin coupling state, inducing superconductivity on the two-dimensional triangular lattice in the CoO$_2$ plane, even though the exact mechanism is still unknown. In the Q1D Ca$_3$Co$_2$O$_6$, since the low-spin Co^{3+} ions with $S=0$ weaken the ferromagnetic (FM) 1D interaction along the CoO$_3$ chain, the interchain AF interaction is almost comparable to the 1D-FM interaction. Therefore 2D-AF order appears even at 100 K in Ca$_3$Co$_2$O$_6$ and related Q1Ds.[5,7] Investigating the magnetic coupling in the limit where the magnetic ions are not clearly coupled at all (0D interaction) is thus an interesting avenue of research to pursue.

Although the rich physics of CoO$_6$ octahedra has been studied extensively, Co ions in CoO$_4$ tetrahedra have at-tracted less attention, because of a relatively small CEF splitting between the e_g and t_{2g} levels in a tetrahedral field. We recently found incommensurate magnetic order in a Co$_3$O$_4$ spinel below $T_N=35$ K, in which only Co^{2+} ions in the tetrahedral sites are responsible for the AF order at low T, by means of positive muon-spin rotation/relaxation (μ^+SR) spectroscopy.[8] Although the origin of the incommensurate magnetic order in spinels is not fully understood, this could suggest charge and/or spin disproportionation of Co ions at the tetrahedral sites.[9] This would also suggest the significance of the relationship between the spin state and the electronic/magnetic structure in materials composed of Co ions in CoO$_4$ tetrahedra. For the Co$_3$O$_4$ spinel, nevertheless, Co^{3+} ions in a low-spin state (i.e., $S=0$) coexist at the octahedral sites, making the interpretation of the underlying mechanism more ambiguous. We thus need to investigate the magnetic nature of materials where Co ions reside *only* in CoO$_4$ tetrahedra.

Recently, Jin *et al.* have grown (by a floating-zone technique) and characterized single-crystal Ba$_2$CoO$_4$ (see Fig. 1),[10] in which the all Co^{4+} ions are in CoO$_4$ tetrahedra. They reported on various structural, electrical, magnetic, and thermal properties of single-crystal Ba$_2$CoO$_4$. In particular, although previous measurements on polycrystalline Ba$_2$CoO$_4$ found no evidence of magnetic order,[11] Jin *et al.* reported Curie-Weiss-like behavior at high temperatures and detected a decrease in χ below $T=25$ K. At such low T, there is magnetic anisotropy—i.e., $\chi(\vec{H}\|\hat{a}) \neq \chi(\vec{H}\perp\hat{a})$. Fitting their susceptibility data to a system with an AF transition, they obtained a Curie-Weiss temperature of $\Theta_p \approx -110$ K with the Co ion sitting in the Co$^{4+}(d^5)$ state with a high-spin value of $S=5/2$.[10] Here it should be noted that, since the CoO$_4$ tetrahedra are isolated from each other—i.e., without connections between nearest neighboring CoO$_4$ tetrahedra, Ba$_2$CoO$_4$ is thought to be a 0D system.
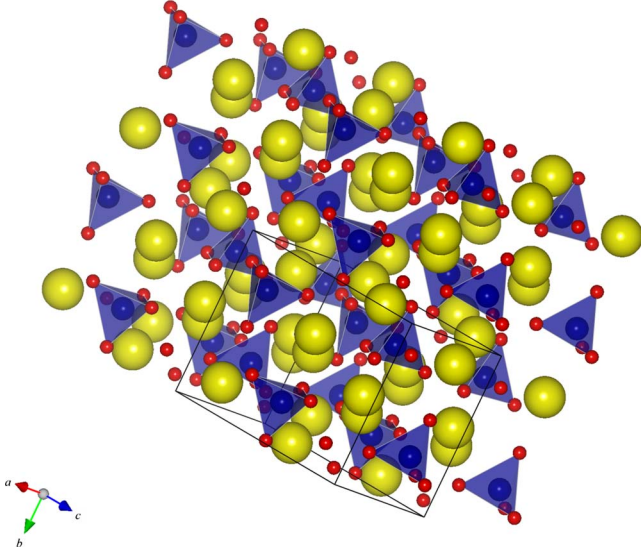
FIG. 1. (Color online) The structure of single-crystal Ba$_2$CoO$_4$, with Ba shown as large spheres (greenish yellow online), O shown as small spheres (red online), and Co shown as medium-sized spheres (blue online). The CoO$_4$ tetrahedra are clearly seen. One of the faces of each tetrahedron is in the *ac* plane. The space group of this monoclinic structure is $P2_1/n$; its lattice parameters are $a=5.9176(13)$ Å, $b=7.6192(16)$ Å, and $c=10.3970(22)$ Å. The structure is very close to being orthorhombic with $\beta_c=91.734°$. Further structural information can be found in Jin *et al.* (Ref. 10).

In order to elucidate the microscopic magnetic nature of Ba$_2$CoO$_4$, we have performed μ^+SR on a single-crystal sample of Ba$_2$CoO$_4$. Because the μ^+ feels the short-range magnetic fields due to its nearest neighbors, μ^+SR spectroscopy is very sensitive to the local magnetic environment, and especially to short-range and/or incommensurate magnetic order, whereas both neutron scattering and susceptibility measurements detect mainly commensurate, long-range, bulk magnetic order; thus μ^+SR is ideally suited to investigate the magnetic properties of Ba$_2$CoO$_4$.

II. EXPERIMENTAL TECHNIQUE

The μ^+SR measurements were carried out on the M20 beamline at TRIUMF, the Canadian National Laboratory located in Vancouver, Canada. M20 provides an intense, highly polarized beam of positive muons. The sample, a 4 mm $\times$ 4 mm $\times$ 11 mm rod of single-crystal Ba$_2$CoO$_4$ (from Oak Ridge) was mounted such that the $\hat{c}$ axis of the crystal faced perpendicular to the muon beam momentum (the initial muon polarization, before spin rotation, being antiparallel to the muon momentum).

Care was taken not to expose the sample to air for any significant length of time, as the sample slowly decomposes by reacting to CO$_2$ and/or moisture. Further sample details can be found in Jin *et al.*[10] For a majority of the measurements, the polarization direction of the in-flight muon was spin rotated via crossed electric and magnetic fields (i.e., a Wien filter), until the initial muon polarization was perpendicular to the beam direction and hence in the same direction
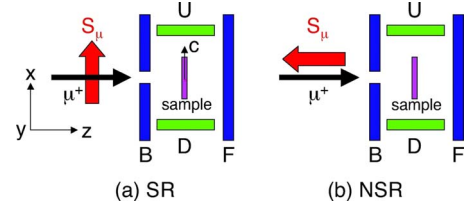
FIG. 2. (Color online) (a) Spin-rotated (SR) experimental setup with crystallographic and muon momentum/polarization directions shown. (b) Non-spin-rotated (NSR) experimental setup.

as the $\hat{c}$-axis direction of the sample. Weak transverse field μ^+SR (wTF-μ^+SR) and zero-field μ^+SR (ZF-μ^+SR) were performed on the sample in the usual way in the spin-rotated (SR) mode unless otherwise noted. The geometry of the experiment can be seen in Fig. 2.

The muon beam has an energy of 4.1 MeV which allows implanted muons to stop several hundred μm into the sample. They constitute a direct *local* probe of magnetism in the bulk of the material. Hence, μ^+SR provides information supplementary to that from other macroscopic probes such as susceptibility (AC susceptibility) and reciprocal space probes (neutron scattering). Further information on μ^+SR techniques can be found in the literature.[12–15]

III. RESULTS

A. wTF-μ^+SR results

In a multiphase sample, the amplitude of the characteristic μ^+SR signal from a given phase is proportional to the volume fraction of that phase. Thus, the muons are not sensitive to small-fraction impurity phases. This can be useful, since magnetic impurities can mask or distort the intrinsic magnetic behavior of a sample in bulk measurements such as susceptibility. With these considerations in mind, wTF-μ^+SR spectra were obtained in a spin-rotated mode between temperatures 20–35 K in an applied field of $H \sim 6$ mT with $\vec{H} \perp \hat{c}$. The μ^+ precession amplitude shows a clear reduction below ~ 25 K as seen in Fig. 3(a). The wTF-μ^+SR spectra were fitted in the time domain with a combination of a slowly relaxing signal precessing at the frequency corresponding to the applied field (due to muons in a paramagnetic environment) and a fast relaxing, nonoscillatory signal due to muons in much larger static local-fields

$$A_0 P(t) = A_{\text{para}} e^{-\lambda_{\text{para}} t} \cos(\omega_\mu t + \phi) + A_{\text{fast}} e^{-\lambda_{\text{fast}} t}, \quad (1)$$

where A_0 is the initial asymmetry, $P(t)$ is the muon spin-polarization function, ω_μ is the muon Larmor frequency ($\omega_\mu = \gamma_\mu H$ with $\gamma_\mu = 2\pi \times 135.54$ MHz/T), ϕ is the initial phase of the precession and A_n and λ_n (n=para, fast) are the asymmetries and exponential relaxation rates of the two signals. The latter signal (n=fast) has a small amplitude above T_N and grows at the expense of the former (A_{para}) below T_N as AF order sets in.

In Fig. 3(b), the magnetic susceptibility is shown parallel and perpendicular to the $\hat{a}$ direction. While the susceptibility perpendicular to $\hat{a}$ is relatively constant in this temperature region, the susceptibility parallel to $\hat{a}$ shows a change at
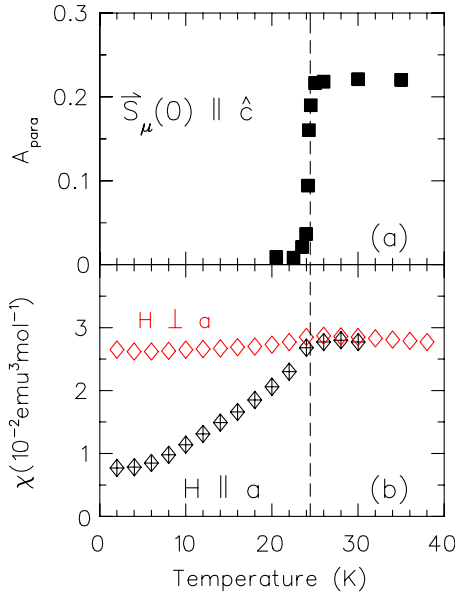
FIG. 3. (Color online) (a) The wTF asymmetry A_{para} plotted as a function of temperature. (b) Temperature dependence of the magnetic susceptibility perpendicular and parallel to the $\hat{a}$ direction, from Jin *et al.* (Ref. 10). A clear transition is seen at $T \approx 24$ K as shown by the dotted line passing through both (a) and (b).

$T \approx 25$ K. This seems to indicate the presence of a magnetic transition with the spins pointing parallel/antiparallel to the $\hat{a}$ direction. As seen in Fig. 3(a), the full wTF-μ^+SR asymmetry A_{para} decreases drastically over a small temperature interval as the sample is cooled below $T \approx 25$ K. The loss of wTF asymmetry is nearly complete at low T, indicating that a magnetic transition is occurring in the entire volume of the sample. This rules out the possibility that the magnetic signal seen in the DC magnetization is due to impurities or defects. The sharpness of the transition seems to indicate the presence of only one magnetic transition occurring throughout the full volume of the sample at about 24 K. This can be contrasted with Fig. 3(b) where the susceptibility changes gradually below 25 K. The transition detected by μ^+SR is very sharp, indicating a second-order phase transition throughout the volume of the sample. The lack of a gradual transition would seem to rule out low-dimensional magnetic interactions as the source of the magnetic order. As the μ^+SR measurement was taken in the spin-rotated mode with the initial spin-polarization $\vec{P}(0) \| \hat{c}$, only field inhomogeneity perpendicular to $\hat{c}$ will dephase the muon-spin polarization. We can take this as confirmation that the internal fields at the muon sites are mostly $\perp \hat{c}$, consistent with spin alignment along $\hat{a}$ as reported by Jin *et al.*[10]

B. ZF-μ^+SR results

Unlike NMR, where a large external magnetic field is usually necessary to sufficiently polarize the nuclear magnetic moments, μ^+SR can be performed in zero applied field since the muon beam is already 100% polarized due to the parity-violating weak decay of the π^+ mesons which generate the muon beam. Thus ZF-μ^+SR is an unique way to
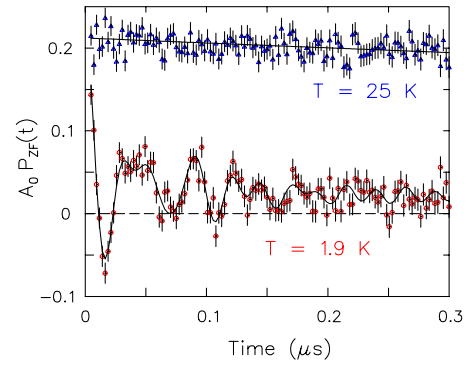
FIG. 4. (Color online) ZF-μ^+SR spectra for Ba$_2$CoO$_4$. Oscillations are clearly seen for $T = 1.9$ K, indicating the presence of specific local magnetic fields at the muon sites. At $T = 25$ K no oscillations are observed, as expected for a sample in the paramagnetic regime.

probe the unperturbed magnetic structure of a sample. We performed ZF-μ^+SR on the Ba$_2$CoO$_4$ sample at temperatures between 1.9 and 30 K. Representative time spectra can be seen in Fig. 4. Here, since the monoclinic structure of Ba$_2$CoO$_4$ is very close to being orthorhombic with $\beta_c = 91.734°$, the effect of the monoclinic distortion on the local-field distribution and directions, which are the main subject in this paper, should be negligibly small.

The asymmetry shows clear multifrequency oscillations below 23 K. This is a strong indication of magnetic order. The low-temperature results were fitted in the time domain assuming that the signal consists of three slowly relaxing precessing signals plus a fast relaxing, nonoscillatory signal and a nonoscillatory signal that describes the slower relaxation of the residual polarization at long times

$$A_0 P_{ZF}(t) = \sum_{n=1}^{3} A_n e^{-\lambda_n t} \cos(\omega_n t + \phi) + A_{fast} e^{-\lambda_{fast} t} + A_{tail} e^{-\lambda_{tail} t},$$

(2)

where A_0 is the initial asymmetry, $P_{ZF}(t)$ is the muon-spin polarization function, ω_n ($n = 1, 2,$ and 3) are the frequencies of the various cosine signals, ϕ is the initial phase of the precession (which is the same for all three frequencies) and A_n and λ_n ($n = 1, 2, 3,$ fast, and tail) are the asymmetries and the exponential relaxation rates of the signals. The last signal ($n =$ tail) is usually expected to be due to nuclear dipolar relaxation. However, this last term has an orientation dependence (see Fig. 6) that is inconsistent with nuclear dipolar relaxation, which is usually more isotropic. We will return to this point later. That the 25 and 1.9 K spectra have basically the same initial asymmetry is evidence that we are not missing any additional magnetic behavior in the sample.

The large asymmetry of the signal in Fig. 5 (top) can be compared to the smaller asymmetry in Fig. 5 (bottom) which is taken in the non-spin-rotated mode (NSR) where $\vec{P}(0) \perp \hat{c}$. This larger asymmetry of the SR signal can also be seen at longer times, as shown in Fig. 6. Since ZF depolarization is caused only by internal fields perpendicular to the initial spin-polarization $\vec{P}(0)$, this further demonstrates that the in-
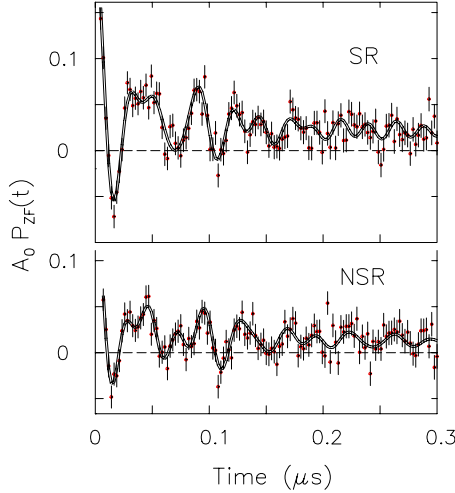
FIG. 5. (Color online) First 300 ns of ZF-μ^+SR spectra at T=1.9 K for data in spin-rotated mode (top) and non-spin-rotated mode (bottom). The larger asymmetry in the SR mode shows that the fields at the muon sites are mainly directed in the *ab* plane of the sample.

ternal fields are predominantly perpendicular to $\hat{c}$. Looking again at Fig. 6, there is a clear orientation dependence of both the initial amplitude A_{tail} and the relaxation rate λ_{tail}, which is nearly a factor of 3 faster for $\vec{P}(0) \perp \hat{c}$ than for $\vec{P}(0) \| \hat{c}$. In general A_{tail} represents the component of the initial muon spin polarization parallel to the local-field direction, which can only relax if there are subsequent fluctuations of the local-field *direction*. Evidently this is much more likely for $\vec{P}(0) \| \hat{c}$, in keeping with the proposition that the local fields are mainly perpendicular to the $\pm \hat{c}$ direction. If λ_{tail} were due primarily to fluctuating nuclear dipole moments, it would be expected to be much more isotropic (and slower).

Figure 7 shows a plot of the real amplitude of the Fourier transforms of ZF-μ^+SR time spectra at temperatures between 1.9 and 25 K. This helps confirm that there are three distinct frequencies that remain distinguishable from one another as the temperature approaches 25 K. Figure 7 also confirms the previous ZF analysis, as we can easily see that the frequency
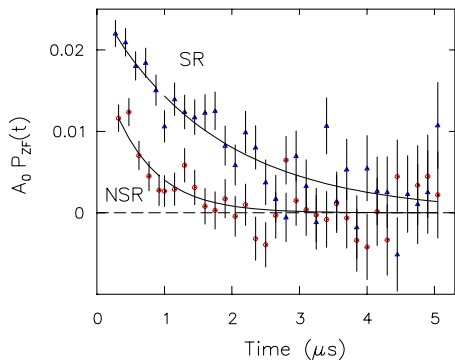
FIG. 6. (Color online) Same spectra as shown in Fig. 5 but shown to longer time scales (5 μs). One can see that the larger asymmetry in the spin-rotated mode also *relaxes* more slowly than the NSR asymmetry.
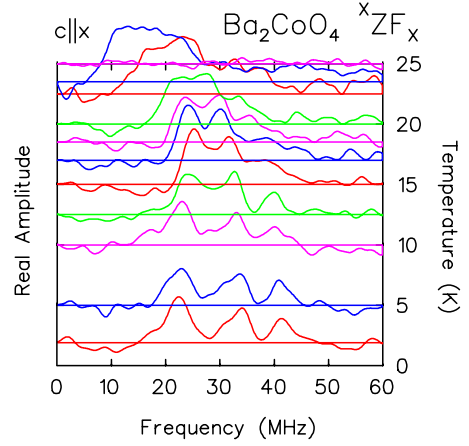
FIG. 7. (Color online) Phase-corrected real amplitudes of the Fourier transforms of the ZF-μ^+SR time spectra plotted as functions of frequency and temperature. All spectra are taken in SR mode. The three frequencies seen in Fig. 8 are clearly distinguishable at low T. As T is increased, each of the three frequencies shifts and broadens until all three disappear at 25 K.

peaks all shift to smaller frequencies together. Thus we eliminate the possibility of missing some more complex behavior of the T dependence of the three signals.

Figure 8 shows the frequencies ($\nu_i \equiv \omega_i / 2\pi$) of the three signals as a function of temperature. All three ν_i have a relatively flat T dependence at low T, whereas as T increases toward 25 K, they start to decrease in magnitude with increasing slope ($d\nu/dT$) and finally drop to zero at T_N. The overall behavior looks similar to that of an order parameter for an AF transition. The details of the $\nu(T)$ curves will be discussed in the next section.

IV. DISCUSSION

A. Dimensionality of the AF transition

The studies of the magnetic structure by Jin *et al.*[10] raise questions regarding the existence or absence of magnetic frustration and/or low-dimensional magnetic interactions, since the Curie-Weiss temperature ($\Theta_p \sim -110$ K) is much larger than $T_N \sim 25$ K. Also, Jin *et al.* note that $\chi(H\|a) \neq 0$ when $T \to 0$ K. This leads to the question of spin canting
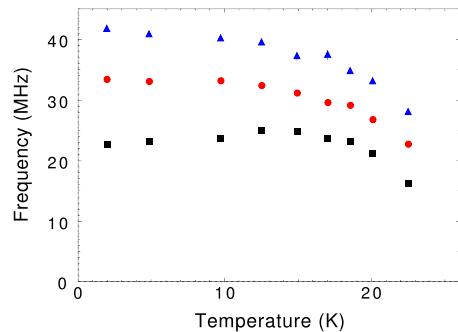
FIG. 8. (Color online) Temperature dependence of the frequencies of the three signals shown in Fig. 7, obtained by fitting the ZF-μ^+SR time spectra to Eq. (2).
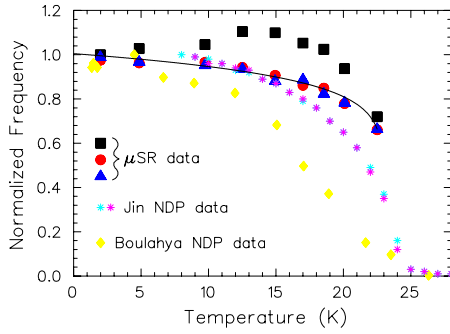
FIG. 9. (Color online) Temperature dependence of the frequencies normalized by their respective $T \rightarrow 0$ frequencies. The solid line represents the result of the fit to Eq. (3).

and/or the existence of defects. As stated above, our wTF results suggest a single second-order phase transition occurring throughout the entire volume of the sample.

The NSR ZF-μ^+SR spectra (Figs. 5 and 6) show precession and hence are interpreted as confirming the existence of a local-field component in the $\hat{c}$ direction. However, the angle between $\vec{B}_{int}$ and the $\hat{c}$ axis is estimated to be $\sim 70°$, which is not inconsistent with the FB counter asymmetry being an artifact of the experimental setup: although the crystal has a definite alignment with the counter geometry, the spin rotation is never exactly 90° in SR mode and is typically $\sim 10-15°$ in NSR mode (because the Wien filter is also used to remove positron contamination from the muon beam). According to neutron results from Sha et al.,[16] spin waves were only observed in the ab plane, diminishing the possibility of some component of the magnetic moment being along the $\hat{c}$ direction. Of course, the local field at a muon site is a microscopic dipolar field, not a bulk magnetization, and so need not be in the same direction as the magnetic moments that produce it.

Figure 9 shows the normalized frequency of each of the three frequencies in the ZF spectra. The two higher frequencies have a similar T dependence fitted by the phenomenological form

$$\nu = \nu_0 (1 - T/T_N)^\beta, \quad (3)$$

where β is the critical exponent. The fit shown as a solid line in Fig. 9 is for a value of $\beta = 0.105(6)$ with a transition temperature of 22.9(1) K. Therefore, although we need more accurate data in the vicinity of T_N to determine β and T_N more precisely and relate the former more conclusively to the dimensionality of the transition, the transition is found to be neither mean-field-like ($\beta = 0.5$) nor a sort of three-dimensional Heisenberg ($\beta = 0.33$). Rather, it is closer to the 2D Ising critical exponent ($\beta = 0.125$) which suggests that reduced-dimensional magnetic interactions are important in the Ba_2CoO_4 system. While not discussed in Ref. 10, the logarithmic behavior they observed in the specific heat is also consistent with the 2D Ising model. More definitely, we can say that all the local muon environments change in roughly the same way. This supports the general conclusion of a *second-order* transition occurring throughout the entire sample.

For the lowest frequency signal (the black squares in Fig. 9), there is a noticeable bump in the $\nu_1(T)$ dependence at ~ 15 K, while the other two signals have a very smooth T dependence.

Neutron powder diffraction from Boulahya et al.[17] shows a marked difference from our results. Even though the transition temperature is roughly the same, the Boulahya results decrease rapidly in the 10–20 K range. Boulahya's NDP experiment was done on a polycrystalline sample; this might be a factor. More recent neutron-scattering results by Jin et al.[16] on a single-crystal sample show a temperature dependence more like that of our data, as shown in Fig. 9.

B. Internal magnetic field(s) in the AF phase

In all the low T fits of the three ν_i, the phase ϕ is consistently close to zero. This strongly suggests that the AF order is commensurate with the crystal lattice, consistent with the clear observation of magnetic Bragg peaks in Ba_2CoO_4 below T_N by a neutron-scattering experiment.[16] Using the relationship $\omega_\mu = \gamma_\mu B$, the internal fields ($B_{int}$) at the three muon sites are estimated to be 166.95 ± 1.4 mT, 247.38 ± 1.4 mT, and 307.53 ± 1.7 mT, respectively, at the lowest T measured.

Recently, two opposing magnetic structures of Ba_2CoO_4 have been proposed. Work by Boulahya et al.[17] suggests that the spins are mostly aligned antiferromagnetically along the c axis with canting out of the ac plane. Their work was primarily based on an elastic neutron-scattering experiment with a powder sample. Sha et al.[16] have proposed a similar magnetic structure but with the spins mostly aligned along the a axis (see Fig. 10). Since μ^+SR is highly sensitive to the local magnetic environment, it should be helpful in distinguishing which AF structure is correct *vis-à-vis* our μ^+SR results.

For this purpose, we first need to determine the muon sites and then perform a dipolar field calculation at those sites. Here a simple electrostatic calculation shows that the muon, when it comes to rest, is located close to the oxygens (which have a charge of −2), much as in the high-T_c cuprate superconductors.[14] Four representative muon sites are shown in Fig. 11, but for the dipolar field calculation below, sixteen muon sites are considered, corresponding to muons located ~ 1 Å away from each oxygen on each tetrahedron.

Next, at each of the muon sites mentioned above, we performed a dipolar field calculation of the magnetic field that would result from the two differing magnetic structures. The dipolar calculation was performed using the following scheme:

$$\vec{B}(\vec{x}_i) = \alpha \sum_{j=1}^{n} \frac{[3(\vec{\mu}_j \cdot \hat{r}_{ij})\hat{r}_{ij} - \vec{\mu}_j]}{r_{ij}^3}, \quad (4)$$

where $\vec{x}_i$ is the location of the ith muon, α is an overall constant, $\vec{\mu}_i$ is the magnetic moment on the jth Co ion and r_{ij} is the distance between the ith muon and the jth Co ion. The sum is taken over 10 unit cells in each crystal direction with the sum converging quite quickly once 5 units cells are considered in each direction. Since the dipolar field drops off as r^{-3}, this quick convergence is expected.
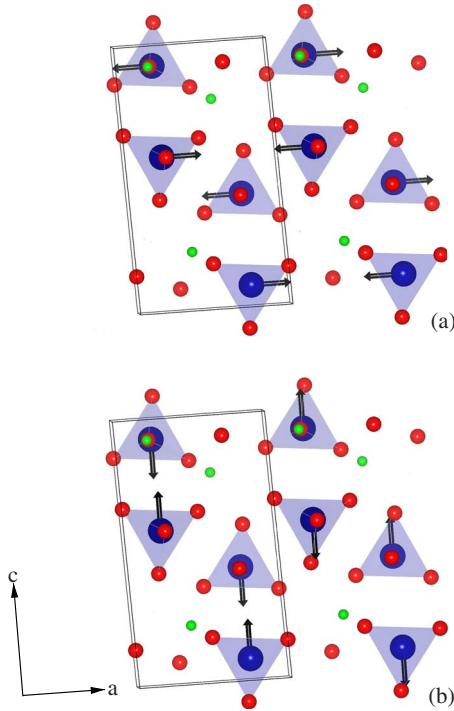
FIG. 10. (Color online) (a) AF magnetic structure (AF*I*) as proposed by Sha *et al.* (Ref. 16). (b) AF magnetic structure (AF*II*) as proposed by Boulahya *et al.* (Ref. 17). Though the magnetic cell is twice the length of the unit cell in both the $\hat{a}$ and $\hat{c}$ directions, only the lower half of the magnetic unit cell is shown, so that the spins can be clearly seen. The CoO_4 tetrahedra are displayed (online) with the Co atoms in blue and the O atoms in red. Each tetrahedron is shaded to help show the crystal structure. The muon sites can be seen (online) as green spheres.

The magnitudes of the fields calculated in this way are shown in Table I for both AF structures. The structure proposed by Boulahya (AF*II*) gives approximately the same
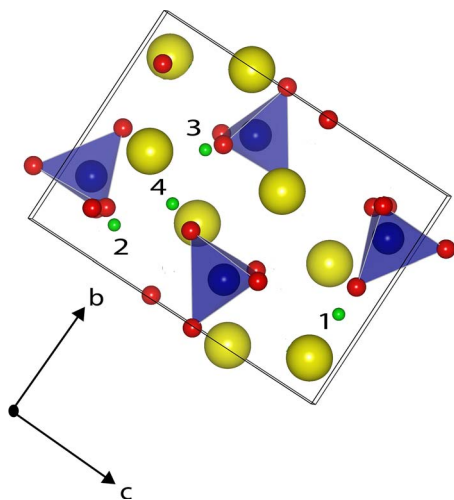
FIG. 11. (Color online) Unit cell, looking down at the *bc* plane in order to clearly show the four representative muon sites as small green (online) spheres. In the dipolar calculation using Eq. (4), each tetrahedron has muon sites 1, 2, 3, and 4; however, for clarity we only show 4 here.

TABLE I. The magnetic field magnitude B_{int} (in mT) at three muon sites (see Fig. 11), as observed for $T \rightarrow 0$ and as calculated using Eq. (4) and the AF structures in Fig. 10(a) [AF*I*] and Fig. 10(b) [AF*II*].

Site	B_{int}^{obs}	Ratio	B_{AFI}^{cal}	Ratio	B_{AFII}^{cal}	Ratio
1	166.9	$\equiv 1$	158.0	$\equiv 1$	253.7	$\equiv 1$
2/3	247.3	1.48	228.1	1.44	268.3	1.06
4	307.4	1.84	290.0	1.84	277.0	1.09

field magnitude ($\pm \sim 5\%$) at each of the four muon sites, whereas for the structure proposed by Sha (AF*I*) all 16 muon sites in one magnetic unit cell see only three different fields, consistent with our ZF-μ^+SR results. Furthermore, while the three fields for the AF*I* structure are all slightly smaller than our experimental values, the *ratios* of the three fields are in surprisingly good agreement with those we observed. Thus AF*I* is much more consistent with our results than AF*II*. We wish to emphasize that μ^+SR is ideally suited to distinguish between the two magnetic structures locally and thus is a very powerful way to gain information on the magnetic structure at the microscopic level. In this sample, with four distinct muon sites, one is able to see the magnetic environment from four unique perspectives. This turned out to be extremely helpful in the above analysis, reinforcing the claim that μ^+SR is an indispensable tool in the study of magnetism.

Ba_2CoO_4 thus seems to have a relatively straightforward AF structure, but there remains the question of why magnetic interactions are lacking along the c axis. At this time there does not seem to be a single satisfactory explanation of how the magnetic moments are actually coupled.

V. SUMMARY

We have observed a sharp magnetic transition in a single crystal of Ba_2CoO_4 via wTF-μ^+SR measurements. From the wTF asymmetry we find that the whole sample enters into a magnetic phase below $T \sim 25$ K. Subsequent ZF-μ^+SR measurements clearly show the existence of static magnetic order for $T < 23$ K. The ZF-μ^+SR spectra also confirm commensurate AF order below T_N. The T-dependence of the ZF signals is consistent with an AF transition of the 2D-Ising type, although the CoO_4 tetrahedra are well isolated from each other. The reduced frequencies all go to zero together with a similar T dependence, which indicates that all muons see magnetic environments governed by the same interactions. Finally, thanks to the power of μ^+SR to probe the local magnetic environment, we can verify the AF magnetic structure proposed by Sha *et al.* in Ref. 16 where the spins are mostly directed along the $\hat{a}$ direction rather than the $\hat{c}$ direction. Our results, while giving basic information on the magnetic structure, still leave unresolved how the Co ions are coupled together. Thus, this compound continues to represent interesting opportunities for further investigation.

*jess@triumf.ca

[1] S. Yamaguchi, Y. Okimoto, H. Taniguchi, and Y. Tokura, Phys. Rev. B **53**, R2926 (1996).

[2] J. B. Goodenough, *Magnetism and the Chemical Bond* (Interscience-Wiley, New York, 1963).

[3] I. Terasaki, Y. Sasago, and K. Uchinokura, Phys. Rev. B **56**, R12685 (1997).

[4] K. Takada, H. Sakurai, E. Takayama-Muromachi, F. Izumi, R. A. Dilanian, and T. Sasaki, Nature (London) **422**, 53 (2003).

[5] J. Sugiyama, H. Nozaki, Y. Ikedo, K. Mukai, D. Andreica, A. Amato, J. H. Brewer, E. J. Ansaldo, G. D. Morris, T. Takami, and H. Ikuta, Phys. Rev. Lett. **96**, 197206 (2006).

[6] W. Koshibae, K. Tsutsui, and S. Maekawa, Phys. Rev. B **62**, 6869 (2000).

[7] J. Sugiyama, H. Nozaki, J. H. Brewer, E. J. Ansaldo, T. Takami, H. Ikuta, and U. Mizutani, Phys. Rev. B **72**, 064418 (2005).

[8] Y. Ikedo, J. Sugiyama, H. Nozaki, H. Itahara, J. H. Brewer, E. J. Ansaldo, G. D. Morris, D. Andreica, and A. Amato, Phys. Rev. B **75**, 054424 (2007).

[9] A. Krimmel, M. Mücksch, V. Tsurkan, M. M. J. Koza, H. Mutka, C. Ritter, D. V. Sheptyakov, S. Horn, and A. Loidl, Phys. Rev. B **73**, 014413 (2006).

[10] R. Jin, Hao Sha, P. G. Khalifah, R. E. Sykora, B. C. Sales, D. Mandrus, and Jiandi Zhang, Phys. Rev. B **73**, 174404 (2006).

[11] G. A. Candela, A. H. Kahn, and T. Negas, J. Solid State Chem. **7**, 360 (1973).

[12] For a recent review of μ^+SR studies in physics and chemistry and technical aspects of μ^+SR, see *Muon Science: Muons in Physics, Chemistry and Materials*, Proceedings of the Fifty First Scottish Universities Summer School in Physics, St. Andrews, August, 1998, edited by S. L. Lee, S. H. Kilcoyne, and R. Cywinski (Institute of Physics, Bristol, 1999).

[13] J. H. Brewer, *Encyclopedia of Applied Physics* (VCH Publishers, New York, 1994), Vol. 11, pp. 23–53.

[14] B. Hitti, P. Birrer, K. Fischer, F. N. Gygax, E. Lippelt, H. Maletta, A. Schenck, and M. Weber, Hyperfine Interact. **63**, 287 (1991).

[15] A. Schenk, *Muon Spin Rotation: Principles and Applications in Solid State Physics* (Adam Hilger, London, 1985).

[16] H. Sha (private communication).

[17] K. Boulahya, M. Parras, J. M. J. González-Calbet, U. Amador, J. L. Martínez, and M. T. Fernámdez-Díaz, Chem. Mater. **18**, 3898 (2006).